DOI: 10.1002/cssc.201200251

Biocatalyzed Artificial Photosynthesis by Hydrogen-Terminated Silicon Nanowires

Hwa Young Lee,[a] Jungki Ryu,[b] Jae Hong Kim,[a] Sahng Ha Lee,[a] and Chan Beum Park*[a]

Semiconductor nanowires have attracted much attention because of their potential for utilizing solar energy. In the field of photovoltaic (or photoelectrochemical) cells that generate electricity (or chemical fuels) from solar conversion, semiconductor nanowires can offer cost-competitive performance compared to conventional planar semiconductor devices.[1–3] Their nanometer-scale dimensions allow for a large surface-to-volume ratio, which increases the number of catalytic reaction sites. Furthermore, the quantum confinement effect enables to tune the semiconductor nanowires' bandgap.[4] Silicon-based nanowires in particular are promising for visible-light-driven photocatalysis with high conversion efficiency for hydrogen production or the degradation of organic pollutants.[5–8] While the absorption of solar energy by bulk silicon is limited because of an indirect bandgap, silicon nanowires have a direct bandgap (a consequence of the quantum confinement effect) that amplifies the photocatalytic conversion efficiency.[9] Nanowires of silicon have advantages over other types of semiconductors, such as TiO_2 and ZnO which can only absorb ultraviolet light (less than 5% of total solar energy) because of their large bandgaps (bulk $E_g \approx 3.2$ eV).[10]

Efficient light-harvesting and utilization of solar energy is also key to natural photosynthesis, which maintains the viability of green plants and photosynthetic bacteria by converting solar energy into chemical energy. In natural photosynthesis, photoexcited electrons originating from photosynthetic reaction centers regenerate chemical reducing power in the form of NAD(P)H, from its oxidized form [i.e., $NAD(P)^+$]. This reducing power is then utilized for the synthesis of hydrocarbons, catalyzed by redox enzymes during the Calvin cycle.[11] Inspired by nature, many efforts have been made to utilize the unlimited source of energythat reaches our planet in the form of solar radiation, by mimicking the natural photosynthetic system.[12] Among the approaches, biocatalyzed artificial photosynthesis is targeted at the photoregeneration of NAD(P)H in vitro from $NAD(P)^+$, and coupling the reducing power to photoenzymatic reactions driven by NAD(P)H-dependent redox enzymes.[13–16] In contrast to inorganic catalysts, NAD(P)H-dependent redox enzymes can accelerate complex synthetic reactions with high specificity and selectivity, using the reducing power provided by the NAD(P)H cofactors.

[a] H. Y. Lee, J. H. Kim, S. H. Lee, Prof. C. B. Park
Department of Materials Science and Engineering
Korea Advanced Institute of Science and Technology
335 Science Road, Daejeon 305-701 (Republic of Korea)
E-mail: parkcb@kaist.ac.kr

[b] Dr. J. Ryu
Department of Materials Science and Engineering
Massachusetts Institute of Technology
77 Massachusetts Avenue, Cambridge, MA 02139 (USA)

In this study, silicon nanowires (SiNWs) are employed as light-harvesting material in biocatalyzed artificial photosynthesis under visible light. We hypothesized that hydrogen-terminated SiNWs (H-SiNWs) may be suitable for biocatalyzed artificial photosynthesis because hydrogen termination on the surface of SiNWs can suppress electron–hole pair regeneration and promote electron transfer.[8] L-Glutamate dehydrogenase (GDH), an NADH-dependent enzyme that can synthesize L-glutamate from α-ketoglutarate, is used as model redox enzyme in this study. As illustrated in Scheme 1, we regenerate NADH

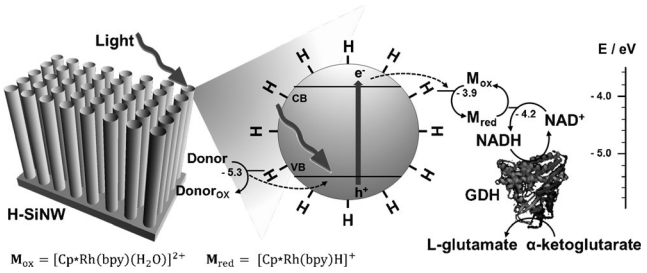

Scheme 1. Illustration and energy-level diagram of biocatalyzed artificial photosynthesis by using hydrogen-terminated silicon nanowires (H-SiNWs) as light-harvesting material. Under illumination of visible light ($\lambda > 420$ nm), H-SiNWs excite electrons from the electron donor and transfer them to NAD^+ via **M**, a rhodium-based electron mediator. The hydrogen termination on the surface suppresses electron–hole pair regeneration and aids the electron transfer. Ultimately, the exicted electrons from reduced NAD^+ (i.e., NADH) are delivered to L-glutamate dehydrogenase (GDH), a redox enzyme, to synthesize L-glutamate from α-ketoglutarate. Redox potentials of the electron donor (i.e., TEOA), **M**, and NAD^+: $E^0(TEOA^+/TEOA) \approx -5.3$ eV, $E^0(\mathbf{M}_{ox}/\mathbf{M}_{red}) <;> -3.9$ eV, $E^0(NAD^+/NADH) \approx -4.2$ eV.

and synthesize L-glutamate by H-SiNWs under irradiation from visible light ($\lambda > 420$ nm). Upon the absorption of energy by H-SiNWs, the photons generate electron–hole pairs by exciting electrons [Equation (1)] taken from an electron donor: triethanolamine [TEOA, Equation (2)]. Excited electrons from H-SiNWs and protons from aqueous solution are transferred to reduce NAD^+ to NADH via a rhodium-based electron mediator, $[Cp^*Rh(bpy)(H_2O)]^{2+}$ [**M**, Equations (3) and (4)].

The use of **M** can prevent the formation of NADH isomers that are inactive in enzymatic reactions.[17] Oxidized **M** (i.e., $\mathbf{M}_{ox}$) accepts two electrons and a proton to form reduced **M** (i.e., $\mathbf{M}_{red}$) [Equation (3)]. The regenerated NADH and additional substrates (ammonium, α-ketoglutarate, and a proton) are used to synthesize L-glutamate by GDH [Equation (5)]. In the electron transfer process, electron-deficient hydrogen atoms on the surface of the H-SiNWs (with a charge of 0.09–0.13 atomic units) act as an electron sink and suppress electron–hole recombination, accelerating the transfer of electrons to the electron acceptor.[8,18] The electrons are employed photo-

chemically to regenerate NADH and drive the synthesis of L-glutamate by GDH.

$$\text{H-SiNWs} \xrightarrow{h\nu} e^- + h^+ \quad (1)$$

$$2\,\text{TEOA} + 2\,h^+ \rightarrow 2\,\text{TEOA}_{ox} \quad (2)$$

$$\mathbf{M}_{ox} + 2\,e^- + H^+ \rightarrow \mathbf{M}_{red} \quad (3)$$

$$\mathbf{M}_{red} + NAD^+ \rightarrow \mathbf{M}_{ox} + NADH \quad (4)$$

$$\alpha\text{-ketoglutarate} + NH_4^+ + NADH + H^+ \xrightarrow{GDH} \text{L-glutamate} + NAD^+ + H_2O \quad (5)$$

We fabricated well-aligned SiNWs through metal-assisted chemical etching, and dipped the as-synthesized SiNWs into dilute hydrofluoric solution to prepare H-SiNWs.[19,20] No morphological change was observed after hydrogen termination of SiNWs according to scanning electron microscopy (SEM) images of vertically aligned H-SiNWs on Si wafer. The diameter of the H-SiNWs was in the range of 100-200 nm, and the length was approximately 20 μm (Figure 1 A). According to transmission electron microscopy (TEM) analysis, the H-SiNWs had a rough surface that was formed by simultaneous lateral etching on the defect sites of the SiNW sidewalls during vertical etching-down (Figure 1 B).

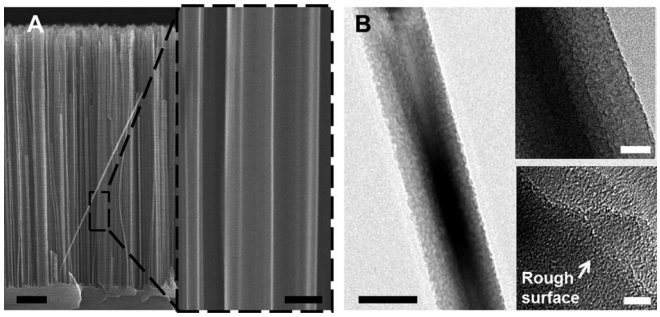

Figure 1. (A) SEM images of H-SiNWs. The inset shows the corresponding magnified image. The length of the H-SiNWs is approximately 20 μm and the diameter is in the range of 100–200 nm. The scale bars for the SEM images are 2 μm (left) and 200 nm (right), respectively. (B) TEM images of H-SiNWs. Insets are high-resolution TEM images of the edge of the H-SiNWs, showing the rough surface. The scale bars are 100 nm (left), 40 nm (upper right), and 4 nm (lower right), respectively.

We tested the photo-regeneration of NADH by using different silicon-based materials: hydrogen-terminated bulk silicon (H-Si), SiNWs, and H-SiNWs (Figure 2 A). Each sample was immersed in a buffer solution containing TEOA, **M**, and NAD^+ and irradiated with visible light. Satisfying our hypothesis, the efficiency of NADH regeneration by H-SiNWs was approximately 80%, which was much higher than that of SiNWs (ca. 10%) and H-Si (ca. 0%). By coupling the H-SiNW-driven photoregeneration of NADH to the redox enzymatic reaction mediated by GDH, we successfully synthesized L-glutamate from α-ketoglutarate: 1.4 mM of L-glutamate was produced after 4 h of reaction with H-SiNWs (Figure 2 B). In contrast, only negligible amounts of L-glutamate were obtained from reactions with

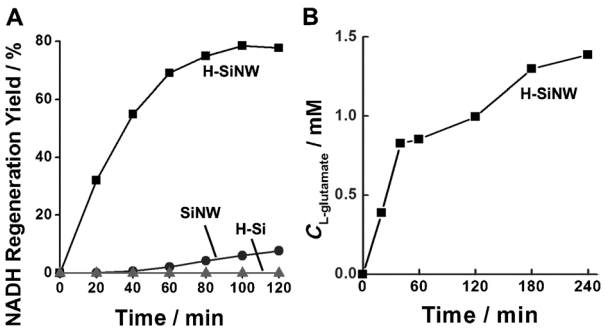

Figure 2. Time profiles for NADH photoregeneration and L-glutamate photosynthesis by GDH. (A) Temporal change of NADH photoregeneration by ■ H-SiNWs, ● SiNWs, and ▲ H-Si . NADH is the final product in the experiment. (B) Photoenzymatic synthesis of L-glutamate from α-ketoglutarate coupled with NADH regeneration by H-SiNWs.

either SiNWs or H-Si (data not shown). We attribute the significant difference in the efficiency of NADH photo-regeneration by SiNWs and H-SiNWs to the hydrogen termination at the surface of the SiNWs. First of all, H-Si could not regenerate NADH because the conduction band (CB) and valence band (VB) edges of H-Si ($E_{CB} \approx -4.0$ eV, $E_{VB} \approx -5.1$ eV)[21] are not suitable for achieving the oxidation of TEOA [$E^0(\text{TEOA}^+/\text{TEOA}) \approx -5.3$ eV][22] or the reduction of both **M** [E^0 ($\mathbf{M}_{ox}/\mathbf{M}_{red}$) ≈ -3.9 eV][17] and NAD^+ [E^0 (NAD^+/NADH) ≈ -4.2 eV],[23] as illustrated in Scheme 1. Nanocrystals on the rough surface of H-SiNWs are known to prompt the effect of quantum confinement and thereby widen the bandgap.[24] The nanocrystals enlarge the band gap of H-SiNWs to 1.45–1.6 eV,[24] increasing E_{CB} and lowering E_{VB} through quantum confinement.[25] From literature data ,[24,25] the energy value of each band is estimated to be approximately E_{CB}: $-3.7 \sim -3.9$ eV and E_{VB}: $-5.3 \sim -5.4$ eV. The enlarged bandgap of the H-SiNWs should thermodynamically enhance electron transfer from TEOA to NAD^+ via **M**.

We investigated the optical, photochemical, and electrochemical properties of SiNWs and H-SiNWs in order to study the effect of hydrogen termination on NADH photoregeneration and biocatalyzed synthesis. Because the electron transfer from TEOA to NAD^+ is triggered by light absorption, the photochemical properties of SiNWs and H-SiNWs in the visible-light range are essential to mimicking natural photosynthesis. The absorption spectra in Figure 3 A indicate that both types of silicon nanowires are visible-light active. SiNWs exhibited higher intensity over all wavelengths than H-SiNWs, which is attributed to a thin native oxide layer on the surface of the SiNWs, which acts as an antireflective layer that enhances visible-light absorption according to the literature.[26,27] To compare the photochemical properties of H-SiNWs to those of SiNWs, we measured the photocurrent from each material under an applied potential of 0.3 V and light irradiation ($\lambda >$ 420 nm). According to our results (Figure 3 B), a lower anodic photocurrent was observed for SiNWs when compared to H-SiNWs, which indicates a less-efficient electron transfer to SiNWs from the electron donor (i.e., TEOA). We attribute the suppressed photochemical properties of SiNWs to the presence of an oxide layer (e.g., SiO_2) on the surface, because the

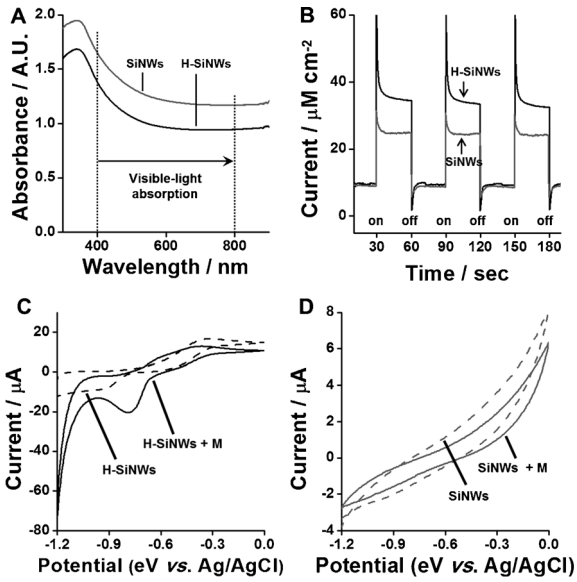

Figure 3. Optical, photochemical, and electrochemical characteristics of H-SiNWs and SiNWs. (A) Optical properties of H-SiNWs and SiNWs measured by UV-visible spectroscopy across wavelengths of 300-900 nm. (B) Photocurrent observed by an applied potential of 0.3 V under irradiation by a 450 W Xe-lamp with a 420 nm cut-off filter. (C,D) Electrochemical characteristics measured by cyclic voltammetry in a phosphate buffer (100 mM, pH 7.5) with (solid line) or without (dotted line) 250 μM **M** at a scan rate of 50 mV s^{-1}. We used a 3-electrode system consisted of a platinum wire as a counter electrode, Ag/AgCl as a reference electrode, and H-SiNWs (or SiNWs) as a working electrode.

oxide layer can lower the electron transfer rate due to its wide band gap and insulating properties.[28] We further observed electrochemical characteristics of H-SiNWs and SiNWs, and their interactions with **M** by using cyclic voltammetry. The reduction potential of **M** was observed at −0.76 V (vs. Ag/AgCl) and the cathodic current of **M** at the reduction potential significantly increased in the presence of H-SiNWs (Figure 3C), suggesting rapid electron transfer to **M** in solution from highly active surface of the electrode, H-SiNWs. Compared to H-SiNWs, the cyclic voltammogram for bare SiNWs showed little or no cathodic current of **M** (Figure 3D), indicating that electrochemically inactive SiO_2 on the surface of SiNWs suppressed electron transfer. Considering that NADH is photochemically regenerated by electron transfer via **M**, the clear cathodic current of **M** is further evidence of efficient NADH photo-regeneration by H-SiNWs.

In order to study further the effect of hydrogen termination on biocatalyzed photosynthesis, we prepared H-SiNWs that had varying degrees of hydrogen termination by annealing H-SiNWs at different temperatures ranging from room temperature to 600 K. Hydrogen atoms bonded to a Si surface are known to coexist in three different types of hydride configurations: monohydride (SiH), dihydride (SiH_2), and trihydride (SiH_3).[29,30] Each configuration has different vibrational stretch modes: monohydrides by M1, M2, and M3, dihydrides by D1 and D2, and trihydrides by T.[29] After annealing H-SiNWs at escalating temperatures, we recorded the vibrational spectra of H-SiNWs in the frequency range of Si–H stretching modes and correlated them to the yield of NADH photo-regeneration (Figure 4). As the annealing temperature increased, the intensity of the absorption peaks from dihydrides and trihydrides (i.e., D1, D2, T) decreased dramatically (Figure 4A) and the

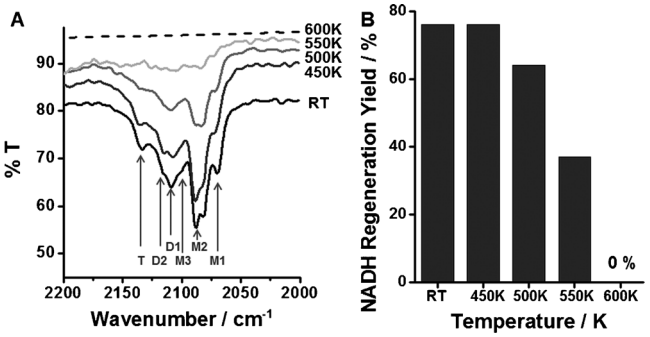

Figure 4. FTIR spectra and NADH regeneration by H-SiNWs annealed at different temperatures. (A) FTIR spectra in the frequency range of Si-H stretching modes of H-SiNWs, annealed from room temperature up to 600 K. The absorption peaks of monohydrides (M1, M2, and M3) are 2070, 2085, and 2099 $cm^{-1,}$ respectively. Dihydrides (D1 and D2) are placed at 2102 and 2110 cm^{-1}, and trihydride (T) is at 2137 cm^{-1}. (B) Comparison of the yields of NADH regeneration by H-SiNWs annealed at different temperatures.

NADH photoregeneration yield was reduced as well (Figure 4B). AT 600 K, no NADH was regenerated, as all the hydrides had disappeared. These results show that hydrogen termination on the surface of H-SiNWs is critical for the efficient photoregeneration of NADH. Taken together, H-SiNWs are suitable for performing highly efficient biocatalyzed artificial photosynthesis under visible light due to their unique photocatalytic properties.

In summary, we successfully applied H-SiNWs as an efficient light-harvesting material for biocatalyzed artificial photosynthesis. Approximately 80% of NADH was regenerated from NAD^+ by H-SiNWs within 2 h of light irradiation ($\lambda > 420$ nm), which is superior to SiNWs (ca. 10%) and H-Si (ca. 0%). The effect of hydrogen termination was confirmed by annealing H-SiNWs at temperatures up to 600 K and applying them to NADH regeneration; as the annealing temperature increased, both the hydrogen termination and the NADH regeneration yield decreased. In addition to the hydrogen termination, an enlarged band gap of H-SiNWs from the effect of quantum confinement facilitated the cascading, photo-induced electron transfer from TEOA to NAD^+ via **M**. Our work shows that H-SiNWs possess high photocatalytic activity that is suitable for the visible light-driven regeneration of NADH and photoenzymatic synthesis.

Experimental Section

Materials: All chemicals, including hydrofluoric acid (HF), silver nitrate ($AgNO_3$), hydrogen peroxide (H_2O_2), nitric acid (HNO_3), β-nicotinamide adenine dinucleotide hydrate (NAD^+), triethanolamine (TEOA), ammonium sulfate [$(NH_4)_2SO_4$], glutamate dehydrogenase (GDH), and α-ketoglutarate, were purchased from Sigma–Aldrich (USA). Lightly doped, n-type silicon (100) was obtained from Tasco

(Korea). The rhodium complex $[Cp^*Rh(bpy)(H_2O)]^{2+}$, **M**, was synthesized according to the literature.[31,32]

Synthesis of silicon nanowires: Silicon nanowires were synthesized by the metal-assisted chemical etching method according to the literature.[19,20] Briefly, a silicon wafer was cut to a size of 10 mm × 40 mm and cleaned with acetone, ethanol, and piranha solutions for 5 min each. The cleaned silicon wafer was rinsed with deionized water several times and immersed in 5% HF solution for 1 min. Then, the wafer was placed into a solution of $AgNO_3$ (5 mM) and HF (4.8 M) for 3 min to deposit silver nanoparticles onto the wafer. Silver nanoparticles on the wafer surface etched down the wafer vertically in a solution of H_2O_2 (0.4 M) and HF (4.8 M). The wafer was etched for 40 min at room temperature. The length of the silicon nanowires could be controlled by changing etching time, H_2O_2 concentration, and temperature. After sufficient etching, the silver nanoparticles were removed by bathing in a dilute nitric acid solution. The as-synthesized silicon nanowires were immersed in a 5% HF solution for hydrogen termination. When annealing H-SiNWs, H-SiNWs were placed in a box furnace(TMO, USA) at specified temperature for 15 min.

NADH photoregeneration and biocatalytic photosynthesis: In order to photoregenerate NADH, silicon nanowires were immersed in a phosphate buffer solution (100 mM, pH 7.5) containing 1 mM NAD^+, 250 μM **M**, and 15 *w/v*% TEOA. The working solution (3 mL) was irradiated using a 450 W Xe lamp with a 420 nm cut-off filter for photon excitation. During NADH photoregeneration, the concentrations of NAD^+ and NADH were measured from peak intensities of absorption at 260 nm and 340 nm, respectively. The photoenzymatic reaction with GDH was carried out in a phosphate buffer (100 mM, pH 7.5) with 1 mM NAD^+, 250 μM **M**, 15 *w/v*% TEOA, 40 units GDH, 5 mM α-ketoglutarate, and 0.1 M $(NH_4)_2SO_4$.

Characterization: The morphology of silicon nanowires was observed using an S-4800 field emission scanning electron microscope (Hitachi High-Technologies Co., Japan) and 200 keV field-emission transmission electron microscope (JEOL LTD, Model JEM-2100F, Japan). UV/Vis absorption spectra were measured using a V-650 spectrophotometer (JASCO Inc., Japan). Fourier transform IR spectra were measured using the ATR FT/IR-6100 (JASCO, Japan). A three-electrode system was used to obtain cyclic voltammograms by using a platinum wire as a counter electrode, Ag/AgCl as a reference electrode (0.197 V vs. standard hydrogen electrode), and H-SiNWs (or SiNWs) as a working electrode in a solution of **M** (250 μM) in a phosphate buffer (100 mM, pH 7.5). In order to make the working electrode, H-SiNWs (or SiNWs) were placed on the glass and were connected to a Cu wire using silver paste. Then, H-SiNWs (or SiNWs) and silver paste were covered by insulating epoxy resin except the very area to be exposed. The system was connected to a multi-channel potentiostat/galvanostat (WonATech, Model WMPG1000, Korea), and the cyclic voltammetry was scanned at a rate of 50 $mV\,s^{-1}$. The photocurrent was also measured using the three-electrode system in a solution of 250 μM **M** with 15 *w/v*% TEOA, connected to the multi-channel potentiostat/galvanostat. A potential of 0.3 V was applied while the system was irradiated by a 450 W Xe-lamp with a 420 nm cut-off filter.

Acknowledgements

This study was supported by grants from the National Research Foundation (NRF) via National Research Laboratory (R0A-2008-000-20041-0), Intelligent Synthetic Biology Center of Global Frontier Project (2011-0031957), Engineering Research Center (2012-0001175), and Converging Research Center (2009-0082276).

Keywords: artificial photosynthesis · biocatalysis · light-harvesting materials · nanowires · silicon

[1] A. I. Hochbaum, P. Yang, *Chem. Rev.* **2010**, *110*, 527 – 546.
[2] M. J. Bierman, S. Jin, *Energy Environ. Sci.* **2009**, *2*, 1050 – 1059.
[3] K. Q. Peng, S. T. Lee, *Adv. Mater.* **2011**, *23*, 198 – 215.
[4] J. Liqiang, S. Xiaojun, S. Jing, C. Weimin, X. Zili, D. Yaoguo, F. Honggang, *Sol. Energy Mater. Sol. Cells* **2003**, *79*, 133 – 151.
[5] I. Oh, J. Kye, S. Hwang, *Nano Lett.* **2012**, *12*, 298 – 302.
[6] Y. Hou, B. L. Abrams, P. C. K. Vesborg, M. E. Björketun, K. Herbst, L. Bech, A. M. Setti, C. D. Damsgaard, T. Pedersen, O. Hansen, J. Rossmeisl, S. Dahl, J. K. Nørskov, I. Chorkendorff, *Nat. Mater.* **2011**, *10*, 434 – 438.
[7] Y. Qu, X. Zhong, Y. Li, L. Liao, Y. Huang, X. Duan, *J. Mater. Chem.* **2010**, *20*, 3590 – 3594.
[8] M. Shao, L. Cheng, X. Zhang, D. D. D. Ma, S. T. Lee, *J. Am. Chem. Soc.* **2009**, *131*, 17738 – 17739.
[9] M. Nolan, S. O'Callaghan, C. Fagas, J. C. Greer, *Nano Lett.* **2007**, *7*, 34 – 38.
[10] J. Zhang, G. Chen, D. W. Bahnemann, *J. Mater. Chem.* **2009**, *19*, 5089 – 5121.
[11] J. Barber, B. Andersson, *Nature* **1994**, *370*, 31 – 34.
[12] D. Gust, T. A. Moore, A. L. Moore, *Acc. Chem. Res.* **2009**, *42*, 1890 – 1898.
[13] J. H. Kim, M. Lee, J. S. Lee, C. B. Park, *Angew. Chem.* **2012**, *124*, 532 – 535; *Angew. Chem. Int. Ed.* **2012**, *51*, 517 – 520.
[14] S. H. Lee, D. H. Nam, J. H. Kim, J. O. Baeg, C. B. Park, *ChemBioChem* **2009**, *10*, 1621 – 1624.
[15] J. K. Ryu, S. H. Lee, D. H. Nam, C. B. Park, *Adv. Mater.* **2011**, *23*, 1883 – 1888.
[16] D. H. Nam, S. H. Lee, C. B. Park, *Small* **2010**, *6*, 922 – 926.
[17] F. Hollmann, B. Witholt, A. Schmid, *J. Mol. Catal. B* **2002**, *19 – 20*, 167 – 176.
[18] R. Q. Zhang, W. C. Lu, Y. L. Zhao, S. T. Lee, *J. Phys. Chem. B* **2004**, *108*, 1967 – 1973.
[19] K. Peng, Y. Yan, S. Gao, J. Zhu, *Adv. Funct. Mater.* **2003**, *13*, 127 – 132.
[20] K. Q. Peng, J. J. Hu, Y. J. Yan, Y. Wu, H. Fang, Y. Xu, S. T. Lee, J. Zhu, *Adv. Funct. Mater.* **2006**, *16*, 387 – 394.
[21] U. Weiler, T. Mayer, W. Jaegermann, C. Kelting, D. Schlettwein, S. Makarov, D. Wolhrle, *J. Phys. Chem. B* **2004**, *108*, 19398 – 19403.
[22] C. Kutal, M. A. Weber, G. Ferraudi, D. Geiger, *Organometallics* **1985**, *4*, 2161 – 2166.
[23] H. K. Chenault, G. M. Whitesides, *Appl. Biochem. Biotechnol.* **1987**, *14*, 147 – 197.
[24] V. A. Sivakov, F. Voigt, A. Berger, G. Bauer, S. H. Christiansen, *Phys. Rev. B* **2010**, *82*, 125446.
[25] R. Q. Zhang, X. M. Liu, Z. Wen, Q. Jing, *J. Phys. Chem. C* **2011**, *115*, 3425 – 3428.
[26] F. Y. Wang, Q. D. Yang, G. Xu, N. Y. Lei, Y. K. Tsang, N. B. Wong, J. C. Ho, *Nanoscale* **2011**, *3*, 3269 – 3276.
[27] W. F. Wu, B. S. Chiou, *Appl. Surf. Sci.* **1997**, *115*, 96 – 102.
[28] P. M. Schneidert, W. B. Fowler, *Phys. Rev. Lett.* **1976**, *36*, 425 – 428.
[29] X. H. Sun, S. D. Wang, N. B. Wong, D. D. D. Ma, S. T. Lee, *Inorg. Chem.* **2003**, *42*, 2398 – 2404.
[30] Y. J. Chabal, G. S. Higashi, K. Raghavachari, S. B. Christman, *Appl. Phys. Lett.* **1988**, *53*, 998 – 1000.
[31] H. Song, S. H. Lee, K. Won, J. H. Park, J. K. Kim, H. Lee, S. Moon, D. K. Kim, C. B. Park, *Angew. Chem.* **2008**, *120*, 1773 – 1776; *Angew. Chem. Int. Ed.* **2008**, *47*, 1749 – 1752.
[32] E. Steckhan, S. Herrmann, R. Ruppert, E. Dietz, M. Frede, E. Spika, *Organometallics* **1991**, *10*, 1568 – 1577.

Received: April 9, 2012
Published online on September 3, 2012

